JOURNAL OF Materials CHEMISTRY
Feature Article

Molecular design and computer simulations of novel mesophases†

Claudio Zannoni

Dipartimento di Chimica Fisica ed Inorganica, Università, Viale Risorgimento 4, 40136 Bologna, Italy. E-mail: Claudio.Zannoni@cineca.it

Received 2nd May 2001, Accepted 18th June 2001
First published as an Advance Article on the web 9th October 2001

The simulation of systems of simple particles interacting through a suitable model potential allows the identification of the essential physical features (anisotropy and biaxiality, electrostatic moments *etc.*) responsible for a certain collective behaviour. Here attractive–repulsive models of the so called Gay–Berne type, that have proved capable of generating nematic, smectic and columnar liquid crystals are described. In particular we discuss the generalization of this simple potential needed to handle biaxial and non-centrosymmetric molecules and we show that by suitable tuning of attractive and repulsive interactions biaxial and polar ferroelectric nematic phases can be obtained in simulations. This could hopefully offer a guide for the design of new mesogenic molecules that are reasonable candidates for the synthesis of these novel mesophases.

1. Introduction

Molecular modeling and computer simulation techniques[1] have recently seen major progresses, due at least in part to the continuous impressive increase in the availability of computer resources and in their performance. Predicting or even reproducing the physical properties and phase transitions of liquid crystals[2] at a molecular level remains, however, a major challenge, with perhaps unique features. A computer simulation approach requires, in general, the setting up of appropriate models for the molecules of interest and the determination by numerical simulation methods[3] of the equilibrium state of a sufficiently large system of N of these particles at the chosen conditions of temperature and pressure. However, differently from the case of ordinary fluids, a simulation of liquid crystal systems should be able to yield the various phases of interest (isotropic, nematic, smectic *etc.*) and their transitions and to provide relevant anisotropic properties (that would reduce to a scalar for normal liquids), for a certain choice of molecular features. This seemingly simple task, that could in principle be carried out starting from atomistic models and force fields, by employing Monte Carlo or molecular dynamics (MD) computer simulation techniques[1,3,4] turns out to be a particularly demanding one when a number of molecules large enough to simulate phase transitions is considered. Moreover, and more relevantly to our present topic, the modeling problem that has to be tackled could be that of designing molecules that have not yet been synthesized and that are good candidates to yield novel mesophases with specific properties of interest for applications. For instance, we could ask about the molecular features that can make a molecule a good candidate to yield the yet unobserved biaxial or ferroelectric thermotropic nematic phases. Alternatively, a problem could be the optimisation of the electric polarization properties of a liquid crystal formed of dipolar molecules and we could be concerned with the effects of changing the position, the orientation and the strength of the permanent dipole on the structure of the liquid crystal phases obtained. In these cases, it is essential to give up as many atomic details as possible and to consider lower resolution models where molecules are approximated with particles of simple shape, as we sketch in Fig. 1, with an emphasis on understanding trends rather than calculating in detail the properties of already known molecules.

A simple choice often made for this purpose is that of adopting purely repulsive models, *e.g.* hard spherocylinders or ellipsoids.[5] This rather extreme choice, consistent with the belief[6] that molecular shape alone determines the structure of a liquid, is appealing for its simplicity but is perhaps more justified for ordered phases obtained with colloidal suspensions[7] than with the materials we are interested here. Indeed, in purely repulsive models[5] temperature plays no direct role, while for thermotropics the change from isotropic to nematic and then to smectic or crystal is temperature driven. In this paper we shall thus concentrate on simple molecular model systems based on particles interacting with attractive–repulsive anisotropic intermolecular potentials,[8] rather than purely repulsive or atomistic models.[9] We shall briefly review the mesophases obtained from the so called Gay–Berne (GB) models[8] and consider the effect of molecular shape and of simple electrostatic contributions, such as dipolar and quadrupolar,

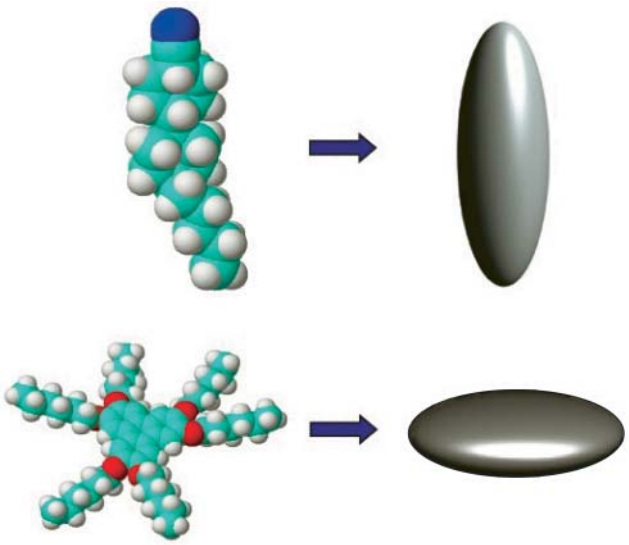

Fig. 1 Atomistic (left) and molecular level (right) models for the elongated and disc-like mesogens. Examples shown: 4′-*n*-pentyl-4-cyanobiphenyl (5CB) (top) and hexa(hexyloxy)triphenylene (bottom).

†Basis of a presentation given at Materials Discussion No. 4, 11–14 September 2001, Grasmere, UK.

DOI: 10.1039/b103923g

in determining phase behaviour. We shall then discuss two examples of novel phases, the biaxial and ferroelectric nematic that have now been obtained in simulations by suitable balance of attractive and repulsive anisotropies with the hope to provide some potentially useful hints for the synthesis.

2. The Gay–Berne potential

Our basic model in this work is the Gay–Berne (GB) potential that represents molecules as uniaxial[8,10–13] or biaxial[14–16] ellipsoids and that can be regarded as a generalized anisotropic and shifted version of the Lennard-Jones (LJ) interaction commonly used for simple fluids,[3] with attractive and repulsive contributions that decrease as 6 and 12 inverse powers of intermolecular distance. In the uniaxial GB model[8] the LJ strength, ε, and range, σ, parameters depend on the orientation vectors $\boldsymbol{u}_i$, $\boldsymbol{u}_j$ of the two particles and on their separation vector $\boldsymbol{r}$:

$$U(\hat{\boldsymbol{u}}_i,\hat{\boldsymbol{u}}_j,\boldsymbol{r}) = 4\varepsilon(\hat{\boldsymbol{u}}_i,\hat{\boldsymbol{u}}_j,\boldsymbol{r})[\{\frac{\sigma_s}{r-\sigma(\hat{\boldsymbol{u}}_i,\hat{\boldsymbol{u}}_j,\hat{\boldsymbol{r}})+\sigma_s}\}^{12} - \{\frac{\sigma_s}{r-\sigma(\hat{\boldsymbol{u}}_i,\hat{\boldsymbol{u}}_j,\hat{\boldsymbol{r}})+\sigma_s}\}^{6}] \quad (1)$$

where the cap indicates a unit vector and the anisotropic contact distance σ is given by

$$\sigma(\hat{\boldsymbol{u}}_i,\hat{\boldsymbol{u}}_j,\hat{\boldsymbol{r}}) = \sigma_s[1-\frac{\chi}{2}\{\frac{(\hat{\boldsymbol{u}}_i\cdot\hat{\boldsymbol{r}}+\hat{\boldsymbol{u}}_j\cdot\hat{\boldsymbol{r}})^2}{1+\chi(\hat{\boldsymbol{u}}_i\cdot\hat{\boldsymbol{u}}_j)} + \frac{(\hat{\boldsymbol{u}}_i\cdot\hat{\boldsymbol{r}}-\hat{\boldsymbol{u}}_j\cdot\hat{\boldsymbol{r}})^2}{1-\chi(\hat{\boldsymbol{u}}_i\cdot\hat{\boldsymbol{u}}_j)}\}]^{-1/2}, \quad (2)$$

The shape anisotropy parameter χ is related to the length σ_e and the breadth σ_s of the ellipsoid representing the molecule:

$$\sigma(\hat{\boldsymbol{u}}_i,\hat{\boldsymbol{u}}_j,\hat{\boldsymbol{r}}) = \sigma_s[1-\frac{\chi}{2}\{\frac{(\hat{\boldsymbol{u}}_i\cdot\hat{\boldsymbol{r}}+\hat{\boldsymbol{u}}_j\cdot\hat{\boldsymbol{r}})^2}{1+\chi(\hat{\boldsymbol{u}}_i\cdot\hat{\boldsymbol{u}}_j)} + \frac{(\hat{\boldsymbol{u}}_i\cdot\hat{\boldsymbol{r}}-\hat{\boldsymbol{u}}_j\cdot\hat{\boldsymbol{r}})^2}{1-\chi(\hat{\boldsymbol{u}}_i\cdot\hat{\boldsymbol{u}}_j)}\}]^{-1/2}, \quad (3)$$

Similarly, the interaction anisotropy is the product of two terms:

$$\varepsilon(\hat{\boldsymbol{u}}_i,\hat{\boldsymbol{u}}_j,\hat{\boldsymbol{r}}) = \varepsilon_o\{1-\frac{\chi'}{2}[\frac{(\hat{\boldsymbol{u}}_i\cdot\hat{\boldsymbol{r}}+\hat{\boldsymbol{u}}_j\cdot\hat{\boldsymbol{r}})^2}{1+\chi'(\hat{\boldsymbol{u}}_i\cdot\hat{\boldsymbol{u}}_j)} + \frac{(\hat{\boldsymbol{u}}_i\cdot\hat{\boldsymbol{r}}-\hat{\boldsymbol{u}}_j\cdot\hat{\boldsymbol{r}})^2}{1-\chi'(\hat{\boldsymbol{u}}_i\cdot\hat{\boldsymbol{u}}_j)}]\}^{\mu} \{1-(\hat{\boldsymbol{u}}_i\cdot\hat{\boldsymbol{u}}_j)^2\chi^2\}^{-\nu/2}, \quad (4)$$

where μ and ν are parameters that can be used to adjust the shape of the potential and

$$\chi' = \frac{\varepsilon_s^{1/\mu}-\varepsilon_e^{1/\mu}}{\varepsilon_s^{1/\mu}+\varepsilon_e^{1/\mu}} \quad (5)$$

reflects the anisotropy in the potential well depths for the side-by-side and end-to-end configurations. The GB potential for a certain choice of parameters is conveniently indicated by the notation GB(χ,χ',μ,ν) proposed by Bates and Luckhurst.[17] Notice that the choice GB(χ,χ',0,0) corresponds to a soft repulsive ellipsoid that has been used in a number of studies,[18] while GB(0,0,μ,ν) reduces to the ordinary spherical LJ potential. It is convenient to employ scaled, dimensionless variables for all quantities, *e.g.* distance $\boldsymbol{r}$ ($r^*=r/\sigma_0$), number density ρ ($\rho^*=N\sigma_0^3/V$), temperature T ($T^*=kT/\varepsilon_0$), energy U ($U^*=U/\varepsilon_0$), pressure P ($P^*=\sigma_0^3P/\varepsilon_0$), viscosity η ($\eta^*=\sigma_0^2\eta/(m\varepsilon_0)^{1/2}$), elastic constants K($K^*=K\sigma_0/\varepsilon_0$) and time t ($t^*=t(\varepsilon_0/m\sigma_0^2)^{1/2}$) that we indicate with an asterisk.

The simulation of the molecular organisation obtained for a system of N model molecules at a certain temperature and pressure (T, P) and the calculation of macroscopic properties typically proceeds through one of the two current mainstream methods of computational statistical mechanics: molecular dynamics (MD) or Monte Carlo (MC).[1,3] MD sets up and solves step by step the equations of motions for all the particles in the system and calculates properties as time averages from the trajectories obtained. MC calculates instead average properties from equilibrium configurations of the system obtained with an algorithm designed to generate sets of positions and orientations of the N molecules with a frequency proportional to their Boltzmann factor. Both methods, although quite different, proceed through repeated evaluations of the energy and thus of the intermolecular interactions in the sample (as well as of their derivatives to evaluate forces, at least in MD). The GB potential with its analytic formulation and its differentiability can be easily coded in both methods. Various parallel implementations of MC[19] and MD[20] simulation codes based on GB potentials, so as to allow particularly large scale simulations, have also been developed and are currently used.[17]

The computer simulation of a set of GB particles with suitable parameterisation leads to a rich variety of liquid crystalline phases. We start by briefly summarizing the results that are obtained from elongated and discotic uniaxial particles and the effects produced on the mesophases by the addition of a permanent dipole or a quadrupole.

3. Elongated uniaxial molecules

The simplest Gay–Berne potential, approximating a molecule with a uniaxial ellipsoid, contains four parameters: σ_e/σ_s, $\varepsilon_s/\varepsilon_e$, μ and ν. Typical parameters used for simulating rod-like molecules (see Fig. 1) are length to breadth $\sigma_e/\sigma_s=3$ and well depth anisotropy $\varepsilon_s/\varepsilon_e=5$. The tuning parameters μ and ν were taken to be 2,1 in the original formulation,[8] by fitting the interaction of two particles consisting of four LJ sites in a row. The corresponding GB(3,5,21,1) potential is strongly anisotropic and favours a side–side alignment, as we can gather from the three sections of the potential surface obtained moving one molecule around one taken at the origin shown in Fig. 2.

The original GB(3,5,2,1) parameterisation is the most thoroughly studied one until now[8,10–13] and both Monte Carlo and molecular dynamics methods have been employed to get the equilibrium phases generated under a variety of thermodynamic conditions and to construct at least in part its phase diagram.[13,21,22] Isotropic, nematic and smectic B

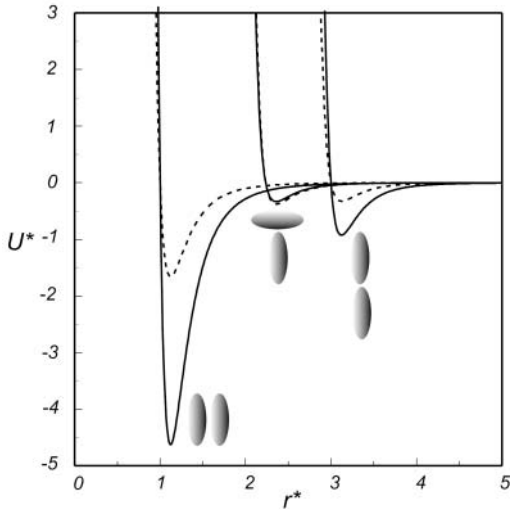

Fig. 2 The GB potential as a function of scaled intermolecular separation for $\sigma_e/\sigma_s=3$, $\varepsilon_s/\varepsilon_e=5$ and energy parameters $\mu=2$, $\nu=1$ (dashed line) and $\mu=1$, $\nu=3$ (continuous line).

Table 1 A summary of the phases observed and of some of the properties studied for systems of elongated particles corresponding to various Gay–Berne parameterisations. Here I, N, S indicate isotropic, nematic, smectic

GB parameters (χ,χ',μ,ν)	Phases observed	Method and comments	Ref.
(3,5,2,1)	I, N, S_B	MD	8,13
		MD viscosity	24
		MD $N=1024$,2048. elastic constants	27–29
(3,5,1,2)	I, N, S	MC, $N=256$	11
(3,5,1,3)	I, N, S_A, S_B	MC (NVT), $N=1000$	34
		MD $N=8000$. elastic constants	28
		MD, $N=8000$, pretransitional effects	35
		MD, $N=65536$. defects	31
(3.0,4,2,1); (3.2,4,2,1); (3.6,4,2,1); (3.8,4,2,1); (3,4,2,1)	I, N, S_A, S_B	Effect of changing the elongation χ MD (NVT), $N=254$ MC (NPT), $N=600$	32
(3,1,1,3); (3,1.25,1,3); (3,2.5,1,3); (3,5,1,3); (3,10,1,3); (3,25,1,3)	I, N, S_A, S_B	Effect of changing attractive well anisotropy χ' MD, $N=256$–864	33
(4.4,20.0,1,1)	I, N, S_A, S_B	N is only observed at high P MC (NPT), $N=2000$; MD (NVT), $N=16000$	17

phases have been found and their order and molecular organization have been studied. A number of physical observables have been determined for GB(3,5,2,1) systems, including translational and rotational correlations,[21–23] viscosity,[24–26] elastic constants,[27–29] thermal conductivity and diffusion coefficients[30] (see Table 1).

The nematic range of the GB(3,5,2,1) system is rather narrow and other parameterisations have been explored. In particular the effect of changing elongation ratio on the phase behaviour and on the dynamics has been studied in refs. 32 and 23.

Keeping the elongation ratio 3 : 1 and potential well anisotropy 5 : 1 and choosing energy parameters $\mu=1$ and $\nu=3$ makes the side–side interaction of two molecules stronger (see Fig. 2) and generates nematics with a wider temperature range.[34] For instance a MC simulation of $N=10^3$ particles in canonical (constant NVT) conditions gives, at a density $\rho^*=0.30$, a nematic–isotropic transition temperature $T_{NI}^*=3.55\pm0.05$ and a nematic–smectic at $T_{SN}^*=2.40\pm0.05$. A snapshot of the molecular organizations obtained at four different temperatures is shown in Fig. 3. An MD study on much larger samples of $N=8000$ particles, which also investigated the pretransitional behaviour of the model, placed T_{NI}^* between 3.45 and 3.50.[35] Typical values for σ_0, ε_0 in real units could be $\sigma_0=\sigma_s=5$ Å, $\varepsilon_0/k=100$ K.

In Fig. 4 we show the second and fourth rank order parameters $\langle P_2\rangle$, $\langle P_4\rangle$ which correspond to the first two moments of the distribution $P(\hat{\boldsymbol{u}}\cdot\hat{\boldsymbol{e}})$ giving the orientation of a molecule with respect to the director $\hat{\boldsymbol{e}}$, as discussed, *e.g.* in ref. 36:

$$< P_2 > = \frac{3}{2} < (\hat{\boldsymbol{u}}\cdot\hat{\boldsymbol{e}})^2 > - \frac{1}{2} \qquad (6a)$$

$$< P_4 > = \frac{35}{8} < (\hat{\boldsymbol{u}}\cdot\hat{\boldsymbol{e}})^4 > - \frac{30}{8} < (\hat{\boldsymbol{u}}\cdot\hat{\boldsymbol{e}})^2 > + \frac{3}{8} \qquad (6b)$$

The results were obtained for a system of GB(3,5,1,3) particles at a scaled density $\rho^*=0.30$.[34] The order parameter is a key quantity in relating to experiment, since it determines the observed anisotropy in second rank tensor properties (*e.g.* diamagnetic susceptivity, refractive index *etc.*). The temperature dependence of $\langle P_2\rangle$ obtained for the GB model is well represented, after subtraction of the small residual order due to the finite sample size, by the Haller type expression often used to fit experimental data:

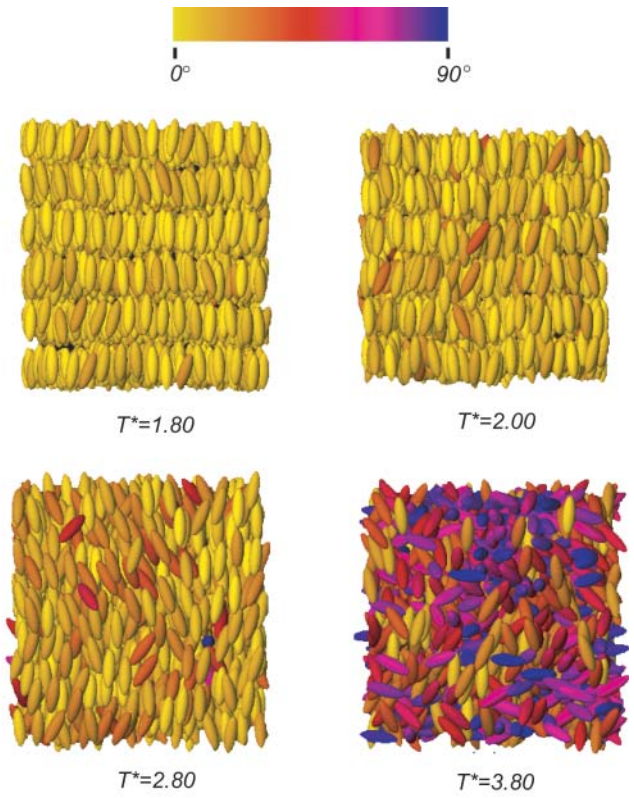

Fig. 3 Typical configurations of a GB(1,3,5,3) model system at four temperatures in the smectic ($T^*=1.80$, 2.00), nematic ($T^*=2.80$) and isotropic ($T^*=3.80$) phase. The colour coding indicates the orientation according to the palette above. Details are given in ref. 34.

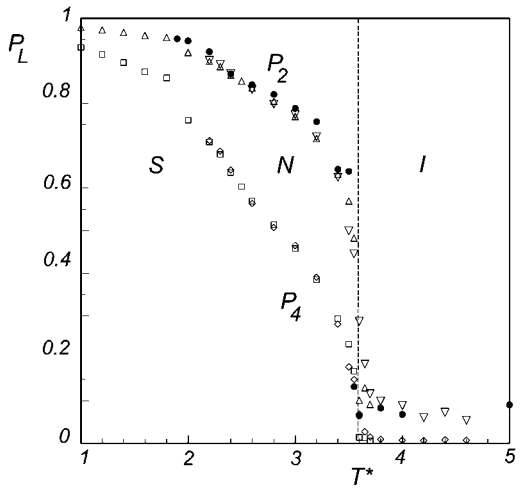

Fig. 4 Order parameters $\langle P_2\rangle$ and $\langle P_4\rangle$ of a GB(3,5,1,3) system as a function of scaled temperature. Details are given in ref. 34.

$$< P_2 > = (1 - \frac{T^*}{T^*_{NI}})^{\beta} \quad (7)$$

The exponent found: $\beta \cong 0.17$, is in very good agreement with the values found for *n*-(4-methoxy benzylidene)-4′-*n*-butylaniline (MBBA) ($\beta \cong 0.174$), other Schiff bases[37] ($0.17 \leqslant \beta \leqslant 0.22$), and for 5CB,[38] $\beta \cong 0.172$. Order parameter data for the GB(3,5,2,1) system can still be fitted as in eqn. (7) but with a larger exponent, *e.g.* for $\rho^* = 0.30$, $\beta \cong 0.37$,[12] corresponding to a much steeper variation of $\langle P_2 \rangle$ with temperature. As another example of the type of problems specific to the simulations of liquid crystals let us briefly consider the study of the nematic–isotropic (NI) phase transition. The NI transition is a first order one, and coexistence is expected, but a flat interface is not observed in simulations of samples with even a relatively large N ($O(10^4)$, say [O = 'order of'] and in consequence even an apparently very simple question about the preferred type of molecular alignment (parallel, perpendicular or tilted) of the particles at the interface is not at all simple to answer. Thus we have studied[39] the molecular organisation at the nematic–isotropic coexistence for a GB(3,5,1,3) model with a specially developed MD method, where the two halves of the cell containing a sufficiently large ($N = 12960$) number of molecules were separately thermostated at temperatures slightly above and below the transition temperature. It was shown that in this case molecules align parallel to the interface. Experimentally this is what happens for some liquid crystals like *n*-(4 methoxybenzylidene)-4′-*n*-butylaniline (MBBA),[40] although a tilted alignment is found for other nematics, *e.g.* for *n*CB.[41] The same MD procedure gave a planar alignment also at the smectic–nematic interface.[42] A planar alignment was also found, with a different simulation technique, by Allen and coworkers[43] in their studies of large length to breadth ratio ($l/d = 15$) GB like ellipsoids, where only the repulsive part of the potential is retained, suggesting that an anchoring tilted away from the surface might be due to additional specific forces.

The effect of the attractive interactions and particularly of the potential well anisotropy χ' on the phase behaviour of the Gay–Berne liquid crystal model for a given value of the molecular elongation $\chi = 3$ was investigated by Allen and coworkers.[33] It was found that smectic order is favoured at lower densities as χ' increases. When χ' is lowered, the smectic phase is pre-empted by the nematic phase which becomes increasingly stable at lower temperatures as χ' is decreased. Liquid–vapour coexistence regions for different values of χ' was found[33] using Gibbs ensemble and Gibbs–Duhem Monte Carlo techniques with an evidence of a vapour–isotropic–nematic triple point when $\chi' = 1$ and $\chi' = 1.25$.[33] This is particularly useful, because it shows that the system presents a nematic–vapour interface (it may be worth mentioning that no liquid–vapour transition is observed with purely repulsive models). The transition of the GB(2,1,3,1.25) model has then been investigated[44,45] and the anchoring at the phase interface has been found to be planar. This is consistent with what is experimentally found for 4,4′-dimethoxyazoxybenzene (PAA),[46] but it should be stated that various types of alignment are found at a free interface: *e.g.* perpendicular in cyanobiphenyls.[47] A perpendicular alignment was actually also observed for a GB system with shorter particles with $\chi = 2$ and $\chi' = 5$, $\mu = 1$, $\nu = 2$.[48]

The interaction of GB liquid crystals with surfaces, particularly with the aim to investigate surface induced ordering and the details of anchoring and structuring,[49] has been explored both for generic[13,50–54] and specific substrates like graphite.[55]

Very large GB systems (from $N = 65536$ for a GB(3,5,1,3) system[56] to even $N = 10^6$ molecules[18] for a soft repulsive model GB(3,–,0,0)) have also been recently studied to investigate some of the most distinctive features of liquid crystals: topological defects,[56,57] until now simulated only with lattice models.[58] In particular, the twist grain boundary phase in smectics[59] and the formation of a variety of defects in nematics by rapid quenching[56] have been examined.

4. Discotic systems

Discotic mesogens[60] can be modelled with oblate GB ellipsoids with thickness σ_f and diameter σ_e (Fig. 1) and nematic and columnar phases have been obtained, although not many studies are available. Luckhurst and coworkers[61] have shown that a GB model based on the dimensions of a triphenylene core, with $\sigma_f/\sigma_e = 0.345$, $\varepsilon_f/\varepsilon_e = 5$, $\mu = 1$, $\nu = 2$ gives an isotropic, nematic and columnar phase with rectangular structure. The simulation of a GB system with the same aspect ratio, but with a parameterisation $\mu = 1$, $\nu = 3$, (Fig. 5) which has the effect of lowering the well depths of the face-to-face and side-by-side configurations gives instead an hexagonal columnar structure,[62,63] as often found in real discotic systems (Fig. 6). A hexagonal non-interdigitated columnar phase was also found[64] with a slightly modified version of the GB potential, where the parameter σ_0 in eqn. (1) was chosen as σ_f, instead of σ_e as in ref. 61

The formation of very ordered columnar structures makes the constant volume simulations troublesome, as indicated by the development of cavities inside the sample. A constant pressure algorithm,[3] where the sample box dimensions and its volume can change has then been employed by various authors to adjust the system to the equilibrium state density.[64]

While order parameters, radial distributions and thermodynamic quantities have been calculated for GB discotics, very few other observables have been determined until now, although in ref. 65 the elastic constants have been determined, *via* a direct pair correlation functions route, and an ordering $K_3^* < K_1^* < K_2^*$, in agreement with experiment, has been found.

One of the potentially interesting applications of columnar materials is their utilization in models for self-assemblying molecular wires,[66] with transmission along the cores and the alkyl chains separating the columns (Fig. 1). Fast energy migration along the column axis has also been experimentally demonstrated by Markovitsi and coworkers in hexakis (*n*-alkoxy)triphenylene compounds, using steady state and time-resolved luminescence.[67] A GB model system has been employed to model energy transfer experiments in columnar phases and to show that the efficiency and directionality of the process increase as the molecular organization changes from isotropic to columnar.[62]

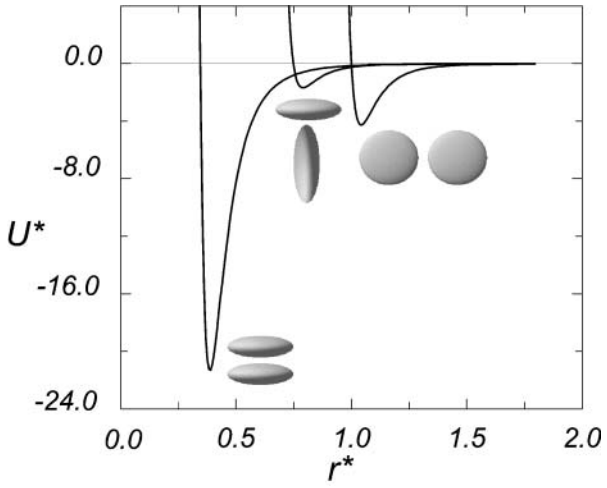

Fig. 5 A GB potential for discotic mesogens for thickness to diameter ratio $\sigma_f/\sigma_e = 0.345$, well depth ratio $\varepsilon_f/\varepsilon_e = 5$ and parameters $\mu = 1$, $\nu = 3$ as a function of intermolecular separation.[62]

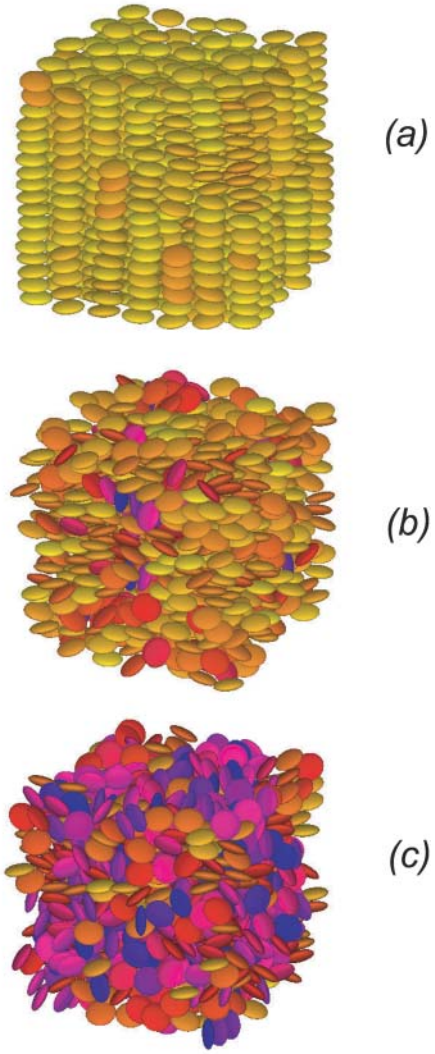

Fig. 6 Molecular organization of ordered phases obtained from GB discs: columnar (a), nematic (b) and isotropic (c). Details are given in ref. 63.

5. Adding dipoles and quadrupoles

We now turn to the effect of adding a dipole and of changing its position and orientation in the molecule on the overall organisation of the dipoles in a liquid crystal phase. Using permanent dipoles as molecular architecture tools is potentially promising, since dipoles are directional, give rise to anisotropic and long range interactions and their position and strength inside the molecule can be "easily" tuned by an appropriate choice of substituents. To investigate these effects, the pair potential to be considered is simply a sum of the Gay–Berne interaction, eqn. (1) and of a dipolar term:

$$U^*_{dd} = \frac{\mu^*_i \mu^*_j}{r^3_d}[\hat{\mu}_i \cdot \hat{\mu}_j - 3(\hat{\mu}_i \cdot \hat{\mathbf{r}}_d)(\hat{\mu}_i \cdot \hat{\mathbf{r}}_d)], \quad (8)$$

where $\mathbf{r}_d$ is the vector joining the point dipoles $\boldsymbol{\mu}_i$ and $\boldsymbol{\mu}_j$ on the two molecules and the scaled dipole $\mu^* = \mu/(\varepsilon_0{}^{1/2}\sigma_0{}^{3/2})$. Notice that while the preferred orientation of two dipoles at a certain distance and orientation can be easily guessed, it is important to stress that the equilibrium organisation of a system of N polar molecules at a certain density and temperature cannot be reliably predicted without the use of computer simulations that optimise the positions and orientations of all the N molecules at the same time. In practice there are a number of cases where a permanent dipole has been added to rod shaped GB models and important modifications have been observed for the molecular organization.[68,19,69–72] The effect of a dipole on mesophase stability depends on its position, orientation and strength, so that a detailed analysis is normally required. In general a terminal axial dipole shifts the nematic–isotropic transition to higher temperatures[68] and a central axial dipole stabilizes the smectic.

As an example we consider[19] the effect of changing the position of an axial dipole from the centre to a distance $d^* = d/\sigma = 1$ towards the end of the molecule (see Fig. 7). We consider a dipole strength $\mu^* = 2$ in reduced units, which would correspond to about 2.4 D in real units.

Considering the same density $\rho^* = 0.30$ used in the previous section for the apolar GB system and confining ourselves to the smectic phase, we find from MC simulations of $N = 1000$ and 8000 dipolar particles that the central dipole system presents an essentially random distribution of up and down dipoles in each layer, with little interdigitation. On the other hand the simulation of the shifted dipole system surprisingly gives the very different striped dipole organisation shown in Fig. 8.

Here at short range the dipoles point in the same direction (same colour here) and are compensated by interdigitation of the layers. Since the dipole is located only on one side of the molecule, the dipole-less end does not interdigitate, giving the structure in Fig. 8. However, the organisation is not a fully bilayer one, but has a stripe domain structure similar to that of the so-called smectic Ã phase that has been found experimentally by Levelut *et al.*[73] in rather complex liquid crystal mixtures. The simple model above helps thus helps to single out a design feature that favours the domain formation, and this is particularly interesting from the perspective of trying to optimise the position of the dipole towards the formation of organized phases.

Changes of dipole strength also have a significant effect and in particular increasing the dipole strength gives rise[72] to the strongly interdigitated partial bilayer smectic A_d[73] phase observed experimentally. GB molecules with transversal dipoles[69] give rise to chains of dipoles in a plane perpendicular to the director, similarly to what has been found in hard spherocylinders with a transverse dipole.[74]

Dipolar effects on GB discs have also been studied using MC simulations for the case of axial[75] and transverse[63] dipoles. For systems with axial dipoles, coherent dipolar domains in the columns have been found, even if these mono-oriented domains do not extend to the whole column. This does not allow formation of ferroelectric columnar systems,[60] that indeed were not observed, but that would be expected for an hexagonal columnar structure with fully polarized columns.[60]

The effects that a quadrupole $\boldsymbol{Q}$ oriented along a direction $\hat{\boldsymbol{a}}$ with respect to the molecular axis has on the mesophase structure and transitions can be studied, adding to the GB

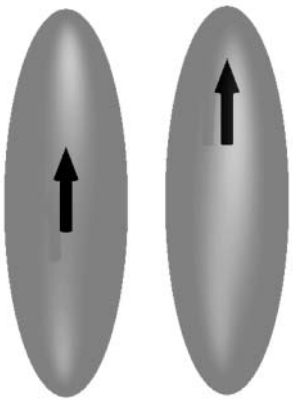

Fig. 7 A sketch of the central (left) and shifted (right) permanent dipole location in the two systems considered. The molecular length is 3σ and the axial dipole is placed at $d = 0$ and 1σ, respectively.

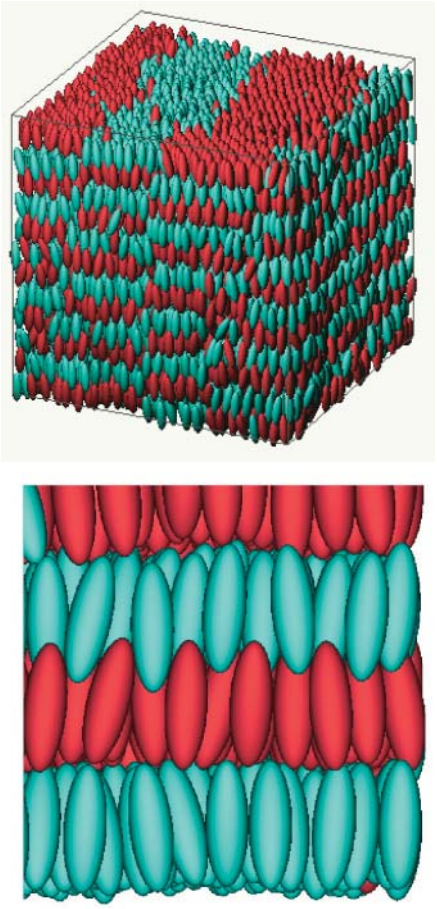

Fig. 8 A snapshot of the smectic Ã striped phase organization obtained for a near terminal axial dipole[19] (top) and a close up of the layer interdigitation (bottom).[19] Red and blue indicate dipole up and down.

potential, eqn. (1) a quadrupole–quadrupole interaction term[76]

$$U^*_{QQ} = \frac{3Q^*_i Q^*_j}{16r^5_q}[1+2(\hat{\boldsymbol{a}}_i\cdot\hat{\boldsymbol{a}}_j)^2-5(\hat{\boldsymbol{a}}_j\cdot\hat{\boldsymbol{r}}_q)^2 -5(\hat{\boldsymbol{a}}_j\cdot\hat{\boldsymbol{r}}_q)^2]-20(\hat{\boldsymbol{a}}_i\cdot\hat{\boldsymbol{r}}_q)(\hat{\boldsymbol{a}}_j\cdot\hat{\boldsymbol{r}}_q) +35(\hat{\boldsymbol{a}}_i\cdot\hat{\boldsymbol{r}}_q)^2(\hat{\boldsymbol{a}}_j\cdot\hat{\boldsymbol{r}}_q)^2], \quad (9)$$

where $\boldsymbol{r}_q$ is the vector joining the point quadrupoles and $Q^* = Q/(\varepsilon_0{}^{1/2}\sigma_0{}^{5/2})$.

In MD simulations of systems of GB(4,5,2,1) with added axial linear quadrupoles, Neal and Parker[77] observed formation of smectic A,B,C phases. They also found that a transverse quadrupole[77] raises the smectic transition temperature and that a large magnitude quadrupole stabilizes the smectic A phase with respect to the Gay–Berne reference fluid. The presence of a large quadrupole seems to stabilize cubic smectic phases rather than the more usual hexagonal smectic B phases.

A problem recently studied is that of mixtures of quadrupolar GB(3,5,1,3) particles with quadrupoles of opposite sign.[78] Suitable mixtures of this type, denoted "magic mixtures" are of great interest as solvents in NMR,[79] in the quest for understanding the ordering mechanism of solutes in liquid crystals. It has been found that the electric field gradient F_{ZZ} experienced by small solutes in this mixtures is zero, leading to the possibility that only solute shape and non-quadrupolar interactions determine alignment. Simulations[78] showed, however, that the compensation effect depends on the size of the quadrupoles and that sufficiently large quadrupoles cause reorganization of the solvent, with F_{ZZ} then depending on both solute and solvent properties.

Quadrupolar discotic GB particles have also been studied[80] both for pure systems and for mixtures of quadrupoles of opposite signs with a view to understand possible mechanisms for the formation of chemically induced columnar liquid crystals.[60] The interaction between quadrupolar discs of opposite sign is strongly attractive for stacked discs and easily leads to column formation.

6. Biaxial systems

While rods and discs correspond to convenient limiting cases of the actual shape of mesogenic molecules and their anisotropy, most molecules will actually have a lower, *e.g.* biaxial symmetry. If we consider a system of lathlike particles we might naively expect them to form a biaxial fluid phase, where molecules tend to align not only their long axis, but also to stack and align their short axis, in addition to (or instead of) a normal uniaxial phase where only the long axis are aligned at long range. The resulting biaxial nematic has indeed been theoretically predicted, at least with approximate mean field type theories over thirty years ago[81] and has been found in lyotropics[82] but to date, notwithstanding a number of claims (see, *e.g.* refs. 83 and 84, and references therein) there is not a universally accepted evidence that the proposed thermotropic phases are indeed biaxial nematics, and actually contrary NMR evidence has been produced on at least some of the candidate materials.[85]

It is therefore particularly stimulating to try and predict some of the key molecular features of a good candidate biaxial mesogen. The first such feature is certainly shape and to a first approximation a biaxial molecule can be treated as an ellipsoid with different semi-axis σ_x, σ_y, σ_z, with an attendant shape biaxiality λ_σ:

$$\lambda_\sigma = \sqrt{\frac{3}{2}}(\sigma_x-\sigma_y)/(2\sigma_z-\sigma_x-\sigma_y) \quad (10)$$

An attempt can then be made to increase λ_σ towards the maximum value $1/\sqrt{6}$ beyond which a distorted rod becomes a distorted disc and some of the proposed molecules, such as 1,4-(*p*-terphenyl)bis[2,3,4-tri(dodecyloxy)benzal]imine studied in ref. 84 approach this limit quite closely, at least in the configuration with fully stretched chains. Optimizing the shape is useful, since as shown by MD simulations of Allen, a system of hard biaxial ellipsoids can generate a biaxial nematic phase.[86] On the other hand in a real thermotropic the potential biaxial phase can only exist in competition with a smectic or crystal phase, that in turn can also be favoured by the same change in shape, and it is thus estimated that only a very small biaxiality window exist.[87] Given the need to fine tune molecular features it is certainly worth considering a biaxial attractive–repulsive potential and generalized GB potentials have been put forward by various authors.[14–16] In a biaxial GB potential the expressions for the core and attractive terms depend on the orientation ω_i, ω_j, ω_r of the two molecules and the intermolecular vector and are necessarily more complicated than those in eqns. (2) and (4). We shall thus not report them here, but we point out that they are still given analytically,[14] which is quite convenient in simulations. For an attractive–repulsive potential it is worth pointing out that we can have different potential wells ε_x, ε_y, ε_z[14–16] for molecules approaching from different directions. These can clearly be treated independently of shape, thus we cannot really talk of a unique biaxiality parameter for a molecule, but we should consider, beyond λ_σ, at least an attractive biaxiality λ_ε, which can be quite different from λ_σ. For a biaxial GB particle λ_ε can be defined as:[14]

$$\lambda_\varepsilon = \sqrt{\frac{3}{2}}(\varepsilon_x^{-1/\mu}-\varepsilon_y^{-1/\mu})/(2\varepsilon_z^{-1/\mu}-\varepsilon_x^{-1/\mu}-\varepsilon_y^{-1/\mu}) \quad (11)$$

We see in Fig. 9 an example of biaxial GB potential[88] with

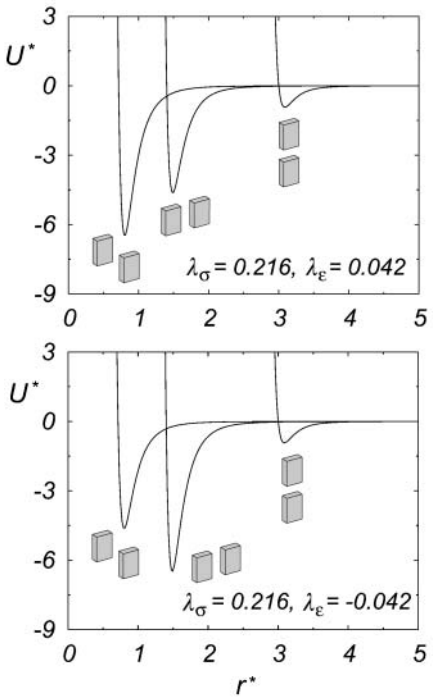

Fig. 9 Biaxial GB potential with shape and attractive biaxiality of opposite sign.[88]

biaxialities of opposite sign. Choosing a negative λ_ε has the effect of energetically disfavouring face-to-face configurations and proved very useful in actually obtaining a thermotropic nematic biaxial phase in our MC simulations.[88]

Using GB particles with $\sigma_x = 1.4$, $\sigma_y = 0.714$, $\sigma_z = 3.0$, which corresponds to biaxialities $\lambda_\sigma = 0.216$ and $\lambda_\varepsilon = -0.06$, together with $\mu = 1$, $\nu = 3$ as discussed in ref. 88 we have found by MC (*NPT*) simulations a biaxial nematic and orthogonal smectic and in Fig. 10 we show snapshots of these two phases as obtained from the simulation. Biaxiality in the sample develops gradually on cooling from the isotropic phase, as we can see from the biaxial order parameter $<R^2_{22}>$ (Fig. 11):

$$< R^2_{22} > = < \frac{1}{4}(1 + \cos^2\beta)\cos 2\alpha \cos 2\gamma - \frac{1}{2}\cos\beta \sin 2\alpha \sin 2\gamma > \quad (12)$$

where (α, β, γ) is the set of Euler angles defining the orientation of a molecule. This orientational order parameter, which is different from zero only if the constituent particles are biaxial

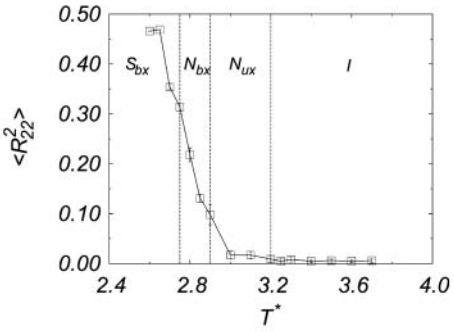

Fig. 11 The biaxial order parameter $<R^2_{22}>$ as a function of temperature for a GB system showing biaxial phases.[88]

and the phase is biaxial is the most convenient one to employ as a monitor of phase biaxiality.[89]

It might be useful for the synthetic chemist to appreciate that tuning both molecular shape and attraction, rather than just shape, can be quite powerful. In practice, a negative attraction biaxiality could be obtained by lateral groups *e.g.*, weak hydrogen bonding sites that favour side-to-side attraction, thus competing with face-to-face stacking.

7. Asymmetric shapes and flexoelectricity

The development of ferroelectric nematic phases, *i.e.* of fluid phases with an overall polar order, is a goal of great fundamental and practical importance.[90,91] Currently known ferroelectric liquid crystal phases are infact relatively complex tilted smectic phases from chiral or from banana-shaped molecules,[91] and these layered phases clearly lack the high fluidity and self healing characteristics that make nematics so useful in electro-optical devices. From a theoretical point of view the existence of a simple uniaxial nematic with polar order is not forbidden[90] but very little is known on the shape and the features that a molecule should present to be a good candidate for exhibiting such a phase. A promising possibility is that of having polyphilic molecules that, thanks to the presence of suitably recognizing groups, favour side-by-side parallel rather than antiparallel ordering.[92]

To investigate molecular models that can yield a polar nematic phase we clearly have to resort to non-centrosymmetric objects, and this goes once more beyond simple GB systems. Complex molecular structures could be simulated by a suitable combination of various ellipsoidal Gay–Berne and spherical Lennard-Jones particles.[93–95] Such an approach, with a simple combination of a sphere and a GB ellipsoid has been

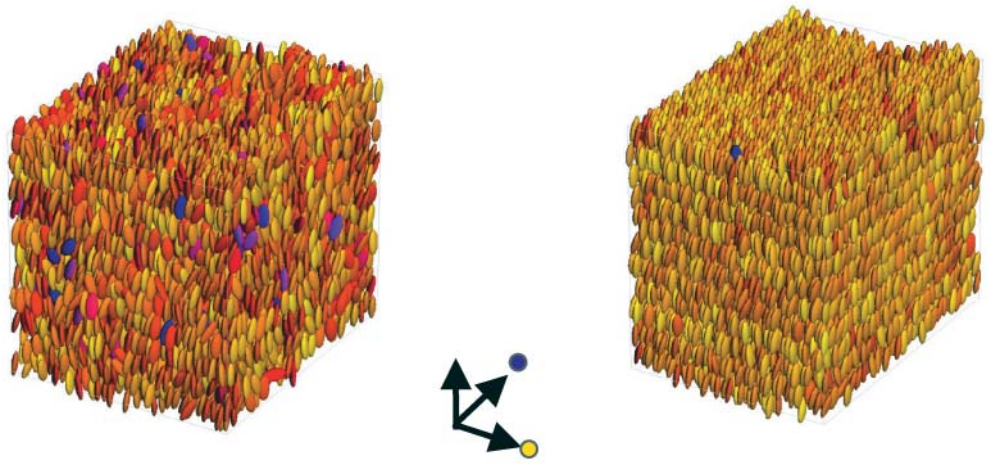

Fig. 10 A snapshot of the biaxial nematic (left) and smectic GB system. The orientations are colour coded with respect to the laboratory axis as shown.[88]

used to model pear shaped molecules and to study flexoelectric effects.[94,95] However, in order to examine the role of molecular shape and of attractive forces in favouring or disfavouring the formation of polar nematics it is more interesting to develop a simple candidate structure that is non-centrosymmetric both in the shape and in the attractive interactions of the two ends of the molecule using a monosite model.

In ref. 96 we have tested the possibility of forming a polar phase with such a model developing a novel attractive–repulsive pair potential for non-centrosymmetric tapered molecules. To do this we have generalized an approach by Zewdie,[97] where $\varepsilon(\omega_1, \omega_2, \omega_r)$ and $\sigma(\omega_1, \omega_2, \omega_r)$ are expanded in terms of rotational invariants, $S(\omega_1, \omega_2, \omega_r)$, functions[98] to obtain non-ellipsoidal monosite interactions.

$$\sigma(w_1,w_2,w_r) = \sum_{L_1L_2L_3} \sigma_{L_1L_2L_3} S^{L_1L_2L_3^*}(w_1,w_2,w_r) \qquad (13)$$

The S functions, introduced by Stone in ref. 38 constitute an orthogonal basis set in the space of the three orientations (ω_1, ω_2, ω_r) and have a relatively simple explicit representation in terms of scalar combinations of powers of the unit vectors defining the orientation of the two molecules and the intermolecular vector.

The core function σ is taken as the contact distance for two particles, considered as rigid objects, which is calculated numerically with a specific algorithm and this is approximated with the series eqn. (13), truncated after a certain number of terms.

Similarly the attractive part of the potential can be expanded and tailored to model a chosen type of attraction, *e.g.* polyphilic attraction between the molecules. We have explored the combined effects of shape and interaction polarity by simulating two model systems formed by tapered shaped molecules (Fig. 12) with centro- and non-centrosymmetric attraction terms.

We have then simulated a system of these tapered molecules[96] using NPT Monte Carlo for a sample of $N=$ 1024 particles.

We find that nematic, polar nematic and smectic phases can be obtained for the second parameterisation, where attractive forces are head-tail discriminating but not for the first parameterization.

In Fig. 13 we show a snapshot of the polar nematic phase obtained and in Fig. 14 a plot of the ordinary second rank order parameter $\langle P_2 \rangle$ and of the polar one $\langle P_1 \rangle$, which is simply:

$$< P_1 > = < (\hat{\boldsymbol{u}}\cdot\hat{\boldsymbol{e}}) > \qquad (14)$$

We see from Fig. 13 that cooling from the isotropic phase the system presents a normal, apolar nematic phase N_a followed by a wide polar nematic N_p and a polar smectic S_p. The polar nematic phase was also stable after introduction of a small axial dipole, thus yielding a ferroelectric nematic.

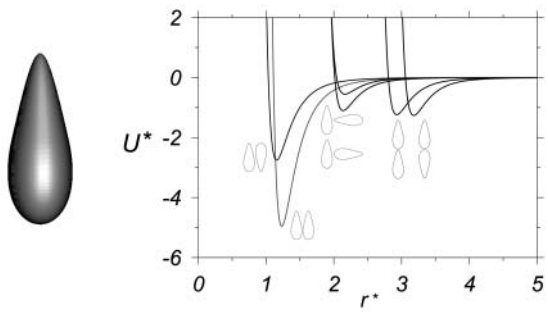

Fig. 12 The 3 : 1 non-centrosymmetric tapered particle with a cone angle of 26° employed in the modelling (left) and the potential between two of these particles (right) for selected approach configurations.[96]

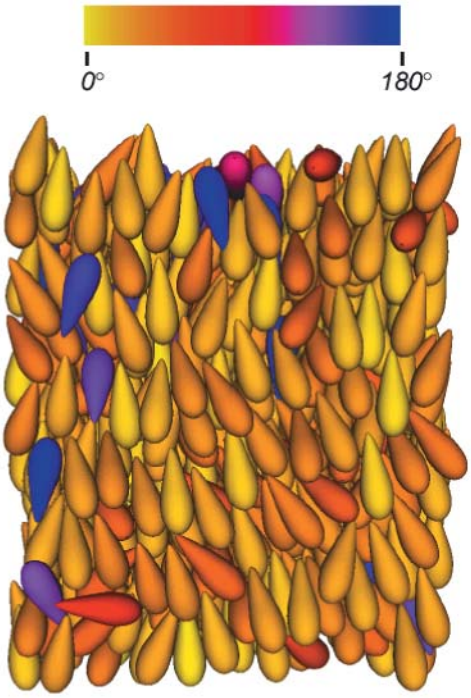

Fig. 13 A snapshot of the polar nematic obtained from tapered molecules. Colour coding for the orientations goes from yellow (up) to blue (down).[96] © Wiley–VCH, 2001.

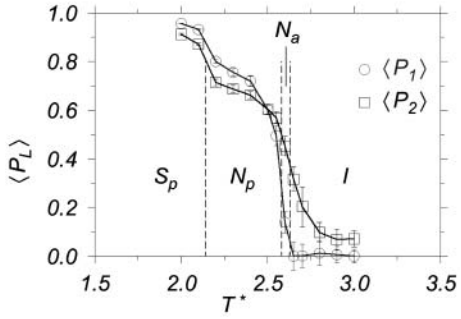

Fig. 14 The polar, $\langle P_1 \rangle$, and non-polar, $\langle P_2 \rangle$, order parameters for the phases obtained from tapered molecules and their temperature dependence. Here I, N_a, N_p, S_p indicate isotropic, apolar nematic, polar nematic and smectic phases.[96]

8. Conclusions

The simple Gay–Berne potential can yield the main liquid crystal phases and their properties and thus constitutes an attractive reference potential for investigating trends of variation in the order and organisation of the nematic and smectic phases under the effect of additional specific contributions, such as molecular dipoles and quadrupoles, as we have summarized here.

We have explored the characteristics that favour the generation of biaxial phases when molecules do not behave decisively as rods or discs. We have discussed attractive and repulsive biaxialities and shown that a thermotropic biaxial nematic can be produced by tuning these two contributions.[19]

We have also introduced some recent generalizations of these Gay–Berne type intermolecular potentials to non-centrosymmetric particles and reported that a system of tapered particles endowed with a suitable directional

attractive interaction can yield ferroelectric nematic and smectic phases.[96] Here too, we find that shape alone does not give the desired polar ordering, pointing to the need of introducing specific attractive contributions.

The simulation of model systems based on simple, molecular level, rather than atomistic, intermolecular potentials thus seems to allow the identification of some of the physical features responsible of a certain collective molecular organization, possibly providing useful guidelines for the design of novel mesogenic molecules and of novel phases.

Acknowledgements

I wish to thank NEDO (Japan), University of Bologna, MURST (PRIN *Cristalli Liquidi*), EU TMR (CT970121), CNR (PF Mat.) for their support and Roberto Berardi, Marco Cecchini, Luca Muccioli, Silvia Orlandi, Paolo Pasini, Matteo Ricci for useful discussions.

References

1 *Advances in the computer simulations of liquid crystals*, ed. P. Pasini and C. Zannoni, Kluwer, Dordrecht, 2000.
2 S. Chandrasekhar, *Liquid Crystals*, 2nd edn., Cambridge University Press, Cambridge, 1992.
3 M. P. Allen and D. J. Tildesley, *Computer Simulation of Liquids*, Clarendon Press, Oxford, 1987.
4 J. Crain and A. V. Komolkin, *Adv. Chem. Phys.*, 1999, **109**, 39.
5 M. P. Allen, G. T. Evans, D. Frenkel and B. M. Mulder, *Adv. Chem. Phys.*, 1993, **86**, 1.
6 H. C. Andersen, D. Chandler and J. D. Weeks, *Adv. Chem. Phys.*, 1976, **34**, 105.
7 S. Fraden, in *Observation, prediction and simulation of phase transitions in complex fluids*, ed.M. Baus, L. F. Rull and J. P. Ryckaert, Kluwer, Dordrecht, 1995.
8 J. G. Gay and B. J. Berne, *J. Chem. Phys.*, 1981, **74**, 3316.
9 M. Wilson, in *Physical Properties of Liquid Crystals, Vol. 1: Nematics*, ed. D. A. Dunmur, A. Fukuda and G. R. Luckhurst, EMIS, IEE, London, 2000, ch. 12.3, p. 63.
10 D. J. Adams, G. R. Luckhurst and R. W. Phippen, *Mol. Phys.*, 1987, **61**, 1575.
11 G. R. Luckhurst, R. A. Stephens and R. W. Phippen, *Liq. Cryst.*, 1990, **8**, 451.
12 J. W. Emsley, G. R. Luckhurst, W. E. Palke and D. J. Tildesley, *Mol. Phys.*, 1992, **11**, 519.
13 (*a*) K. Chalam, K. E. Gubbins, E. de Miguel and L. F. Rull, *Mol. Simul.*, 1991, **7**, 357; (*b*) E. de Miguel, L. F. Rull, M. K. Chalam and K. E. Gubbins, *Mol. Phys.*, 1991, **74**, 405; (*c*) E. de Miguel, L. F. Rull, M. K. Chalam, K. E. Gubbins and F. van Swol, *Mol. Phys.*, 1991, **72**, 593.
14 R. Berardi, C. Fava and C. Zannoni, *Chem. Phys. Lett.*, 1995, **236**, 462; R. Berardi, C. Fava and C. Zannoni, *Chem. Phys. Lett.*, 1995, **297**, 8.
15 G. Ayton and G. N. Patey, *J. Chem. Phys.*, 1995, **102**, 9040.
16 D. J. Cleaver, C. M. Care, M. P. Allen and M. P. Neal, *Phys. Rev. E*, 1996, **54**, 559.
17 M. A. Bates and G. R. Luckhurst, *J. Chem. Phys.*, 1999, **110**, 7087.
18 D. Andrienko, G. Germano and M. P. Allen, *Phys. Rev. E*, 2001, **63**, 041701.
19 R. Berardi, S. Orlandi and C. Zannoni, *Chem. Phys. Lett.*, 1996, **261**, 357.
20 (*a*) M. P. Allen, M. A. Warren, M. R. Wilson, A. Sauron and W. Smith, *J. Comput. Chem.*, 1997, **18**, 478; (*b*) M. Wilson, in *Advances in the computer simulations of liquid crystals*, ed. P. Pasini and C. Zannoni, Kluwer, Dordrecht, 2000; (*c*) J. Ilnytskyi and M. R. Wilson, *Comput. Phys. Commun.*, 2001, **134**, 23.
21 E. de Miguel, L. F. Rull and K. E. Gubbins, *Phys. Rev. A*, 1992, **45**, 3813.
22 L. F. Rull, *Physica A*, 1995, **220**, 113.
23 (*a*) A. Perera, S. Ravichandran, M. Moreau and B. Bagchi, *J. Chem. Phys.*, 1997, **106**, 1280; (*b*) S. Ravichandran, A. Perera, M. Moreau and B. Bagchi, *J. Chem. Phys.*, 1997, **107**, 8469.
24 A. M. Smondyrev, G. B. Loriot and R. A. Pelcovits, *Phys. Rev. Lett.*, 1995, **75**, 2340.
25 L. Bennett and S. Hess, *Phys. Rev. E*, 1999, **60**, 1063; S. Hess, in *Advances in the computer simulations of liquid crystals*, ed. P. Pasini and C. Zannoni, Kluwer, Dordrecht, 2000.
26 S. Cozzini, L. F. Rull, G. Ciccotti and G. V. Paolini, *Physica A*, 1997, **240**, 173.
27 J. Stelzer, L. Longa and H.-R. Trebin, *J. Chem. Phys.*, 1995, **103**, 3098.
28 M. P. Allen, M. A. Warren, M. R. Wilson, A. Sauron and W. Smith, *J. Chem. Phys.*, 1996, **105**, 2850.
29 J. Stelzer, L. Longa and H.-R. Trebin, *J. Chem. Phys.*, 1997, **107**, 1295E.
30 S. Sarman and D. J. Evans, *J. Chem. Phys.*, 1993, **99**, 620.
31 J. L. Billeter, A. M. Smondyrev, G. B. Loriot and R. A. Pelcovits, *Phys. Rev. E*, 1999, **60**, 6831.
32 (*a*) J. T. Brown, M. P. Allen, E. Martín del Río and E. de Miguel, *Phys. Rev. E*, 1998, **57**, 6685; (*b*) J. T. Brown, M. P. Allen and M. Warren, *J. Phys. Condens. Matter*, 1996, **8**, 9433.
33 E. de Miguel, E. M. del Río, J. T. Brown and M. P. Allen, *J. Chem. Phys.*, 1996, **105**, 4234.
34 R. Berardi, A. P. J. Emerson and C. Zannoni, *J. Chem. Soc., Faraday Trans.*, 1993, **89**, 4069.
35 M. P. Allen and M. A. Warren, *Phys. Rev. Lett.*, 1997, **78**, 1291.
36 C. Zannoni, in *The Molecular Physics of Liquid Crystals*, ed. G. R. Luckhurst and G. W. Gray, Academic Press, London, 1979, pp. 51 and 84.
37 F. Leenhouts, W. H. de Jeu and A. J. Dekker, *J. Phys.*, 1979, **40**, 989.
38 S. T. Wu and R. J. Cox, *J. Appl. Phys.*, 1988, **64**, 821.
39 M. Bates and C. Zannoni, *Chem. Phys. Lett.*, 1997, **280**, 40.
40 D. Langevin and M. Bouchiat, *Mol. Cryst. Liq. Cryst.*, 1973, **22**, 317.
41 S. Faetti and V. Palleschi, *Phys. Rev. A*, 1984, **30**, 3241.
42 M. Bates, *Chem. Phys. Lett.*, 1998, **288**, 209.
43 N. Akino, F. Schmid and M. P. Allen, *Phys. Rev. E*, 2001, **63**, 041706.
44 A. P. J. Emerson, S. Faetti and C. Zannoni, *Chem. Phys. Lett.*, 1997, **271**, 241.
45 E. de Miguel and E. M. del Río, *Phys. Rev. E*, 1997, **55**, 2916.
46 M. A. Bouchiat and D. Langevin-Cruchin, *Phys. Lett. A*, 1971, **34**, 331.
47 H. Kasten and G. Strobl, *J. Chem. Phys.*, 1995, **103**, 6768.
48 S. J. Mills, C. M. Care, M. P. Neal and D. J. Cleaver, *Phys. Rev. E*, 1998, **58**, 3284.
49 E. M. Martín del Río, M. M. Telo da Gama, E. de Miguel and L. F. Rull, *Phys. Rev. E*, 1995, **52**, 5028.
50 Z. P. Zhang, A. Chakrabarti, O. G. Mouritsen and M. J. Zuckermann, *Phys. Rev. E.*, 1996, **53**, 2461.
51 (*a*) J. Stelzer, P. Galatola, G. Barbero and L. Longa, *Phys. Rev. E*, 1997, **55**, 477; (*b*) J. Stelzer, L. Longa and H.-R. Trebin, *Phys. Rev. E*, 1997, **55**, 7085.
52 G. D. Wall and D. J. Cleaver, *Phys. Rev. E*, 1997, **56**, 4306.
53 (*a*) T. Gruhn and M. Schoen, *Mol. Phys.*, 1998, **93**, 681; (*b*) T. Gruhn, M. Schoen and D. J. Diestler, *J. Chem. Phys.*, 1998, **109**, 301.
54 T. Miyazaki, H. Hayashi and M. Yamashita, *Mol. Cryst. Liq. Cryst.*, 1999, **330**, 1611.
55 V. Palermo, F. Biscarini and C. Zannoni, *Phys. Rev. E*, 1998, **57**, 2519.
56 J. L. Billeter, A. M. Smondyrev, G. B. Loriot and R. A. Pelcovits, *Phys. Rev. E*, 1999, **60**, 6831.
57 M. P. Allen, M. A. Warren and M. R. Wilson, *Phys. Rev. E*, 1998, **57**, 5585.
58 C. Chiccoli, O. D. Lavrentovich, P. Pasini and C. Zannoni, *Phys. Rev. Lett.*, 1997, **79**, 4401.
59 M. P. Allen, M. A. Warren and M. R. Wilson, *Phys. Rev. E*, 1998, **57**, 5585.
60 D. Guillon, *Struct. Bonding (Berlin)*, 1999, **95**, 41.
61 A. P. J. Emerson, G. R. Luckhurst and S. G. Whatling, *Mol. Phys.*, 1994, **82**, 113.
62 C. Bacchiocchi and C. Zannoni, *Phys. Rev.E*, 1998, **58**, 3237.
63 R. Berardi, S. Orlandi and C. Zannoni, *PCCP*, 2000, **2**, 2933.
64 M. A. Bates and G. R. Luckhurst, *J. Chem. Phys.*, 1996, **104**, 6696.
65 J. Stelzer, M. A. Bates, L. Longa and G. R. Luckhurst, *J. Chem. Phys.*, 1997, **107**, 7483.
66 D. Adam, P. Schuhmacher, J. Simmerer, L. Haussling, K. Siemensmeyer, K. H. Etzbach, H. Ringsdorf and D. Haaerer, *Nature*, 1994, **371**, 141.
67 D. Markovitsi, F. Rigaut, M. Mouallem and J. Malthete, *Chem. Phys. Lett.*, 1987, **135**, 236.

68 K. Satoh, S. Mita and S. Kondo, *Chem. Phys. Lett.*, 1996, **255**, 99.
69 R. Berardi, S. Orlandi and C. Zannoni, *Int. J. Mod. Phys. C*, 1999, **10**, 477.
70 E. Gwóźdź, A. Bródka and K. Pasterny, *Chem. Phys. Lett.*, 1997, **267**, 557.
71 (*a*) M. Houssa, A. Oualid and L. F. Rull, *Mol. Phys.*, 1998, **94**, 439; (*b*) M. Houssa, S. C. McGrother and L. F. Rull, *J. Chem. Phys.*, 1998, **109**, 9529; (*c*) M. Houssa, S. C. McGrother and L. F. Rull, *Comput. Phys. Commun.*, 1999, 259.
72 R. Berardi, S. Orlandi, D. Photinos, A. Vanakaras and C. Zannoni, to be published
73 A. M. Levelut, R. J. Tarento, F. Hardouin, M. F. Achard and G. Sigaud, *Phys. Rev. A*, 1981, **24**, 2180.
74 A. Gil-Vilegas, S. McGrother and G. Jackson, *Chem. Phys. Lett.*, 1997, **267**, 557.
75 R. Berardi, S. Orlandi and C. Zannoni, *J. Chem. Soc., Faraday Trans.*, 1997, **93**, 1493.
76 A. D. Buckingham, *Adv. Chem. Phys.*, 1978, **12**, 107.
77 (*a*) M. P. Neal and A. J. Parker, *Mol. Cryst. Liq. Cryst.*, 1999, **330**, 1809; (*b*) *Chem. Phys. Lett*. 1998, **294**, 277.
78 E. E. Burnell, R. Berardi, R. T. Syvitski and C. Zannoni, *Chem. Phys. Lett.*, 2000, **331**, 455.
79 E. E. Burnell and C. A. de Lange, *Chem. Rev.*, 1998, **98**, 2359.
80 M. A. Bates and G. R. Luckhurst, *Liq. Cryst.*, 1998, **24**, 229.
81 M. J. Freiser, *Phys. Rev. Lett.*, 1970, **24**, 1041.
82 L. J. Yu and A. Saupe, *Phys. Rev. Lett.*, 1980, **45**, 1000.
83 See, *e.g.*, *Oxford Workshop on Biaxial Nematics* , ed. D. Bruce, G. R. Luckhurst and D. Photinos, *Mol. Cryst. Liq. Cryst*., 1998, **323**, 153.
84 S. Chandrasekhar, G. G. Nair, D. S. Shankar Rao, S. K. Prasad, K. Praefcke and D. Blunk, *Curr. Sci.*, 1998, **75**, 1042.
85 S. M. Fan, I. D. Fletcher, B. Guendogan, N. J. Heaton, G. Kothe, G. R. Luckhurst and K. Praefcke, *Chem. Phys. Lett.*, 1993, **204**, 517.
86 (*a*) M. P. Allen, *Mol. Phys.*, 1984, **52**, 717; (*b*) M. P. Allen, *Liq. Cryst.*, 1990, **8**, 499.
87 A. Ferrarini, P. L. Nordio, E. Spolaore and G. R. Luckhurst, *J. Chem. Soc., Faraday Trans.*, 1995, **91**, 3177.
88 R. Berardi and C. Zannoni, *J. Chem. Phys.*, 2000, **113**, 5971.
89 F. Biscarini, C. Chiccoli, P. Pasini, F. Semeria and C. Zannoni, *Phys. Rev. Lett.*, 1995, **75**, 1803.
90 L. M. Blinov, *Liq. Cryst.*, 1998, **24**, 143.
91 D. Guillon, *Adv. Chem. Phys.*, 2000, **113**, 1.
92 F. Tournilhac, L. M. Blinov, J. Simon and S. V. Yablonsky, *Nature*, 1992, **359**, 621.
93 M. P. Neal, A. J. Parker and C. M. Care, *Mol. Phys.*, 1997, **91**, 603.
94 J. Stelzer, R. Berardi and C. Zannoni, *Chem. Phys. Lett.*, 1999, **299**, 9.
95 J. L. Billeter and R. A. Pelcovits, *Liq. Cryst.*, 2000, **9**, 1151.
96 R. Berardi, M. Ricci and C. Zannoni, *ChemPhysChem.*, 2001, **2**, 443.
97 (*a*) H. Zewdie, *J. Chem. Phys.*, 1998, **108**, 2117; (*b*) H. Zewdie, *Phys. Rev. E*, 1998, **57**, 1793.
98 A. J. Stone, *Mol. Phys.*, 1978, **36**, 241.